

NAVY CITE - 1100V



Naval Research Laboratory

Washington, DC 20375-5000

NRL Report 9140

AD-A201 052

Bounds on Doppler Frequency Estimation in Correlated Nonstationary Gaussian Noise

FENG-LING C. LIN AND BEN H. CANTRELL

*Target Characteristics Branch
Radar Division*

August 23, 1988

DTIC
ELECTE
DEC 09 1988
S **D**
CE

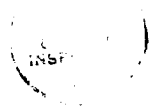
8 8 12 9 039

REPORT DOCUMENTATION PAGE				Form Approved OMB No 0704-0188	
1a REPORT SECURITY CLASSIFICATION UNCLASSIFIED			1b RESTRICTIVE MARKINGS		
2a SECURITY CLASSIFICATION AUTHORITY			3 DISTRIBUTION/AVAILABILITY OF REPORT		
2b DECLASSIFICATION/DOWNGRADING SCHEDULE			Approved for public release; distribution unlimited.		
4 PERFORMING ORGANIZATION REPORT NUMBER(S) NRL Report 9140			5 MONITORING ORGANIZATION REPORT NUMBER(S)		
6a NAME OF PERFORMING ORGANIZATION Naval Research Laboratory		6b OFFICE SYMBOL (if applicable)	7a NAME OF MONITORING ORGANIZATION		
6c ADDRESS (City, State, and ZIP Code) Washington, DC 20375-5000			7b ADDRESS (City, State, and ZIP Code)		
8a NAME OF FUNDING/SPONSORING ORGANIZATION Office of Naval Research		8b OFFICE SYMBOL (if applicable)	9 PROCUREMENT INSTRUMENT IDENTIFICATION NUMBER		
8c ADDRESS (City, State, and ZIP Code) Arlington, VA 22217-5000			10 SOURCE OF FUNDING NUMBERS		
		PROGRAM ELEMENT NO 61153N	PROJECT NO 021-05-43	TASK NO	WORK UNIT ACCESSION NO DN480-006
11 TITLE (Include Security Classification) Bounds on Doppler Frequency Estimation in Correlated Nonstationary Gaussian Noise					
12 PERSONAL AUTHOR(S) Lin, F. C. and Cantrell, B. H.					
13a TYPE OF REPORT Interim		13b TIME COVERED FROM _____ TO _____		14 DATE OF REPORT (Year, Month, Day) 1988 August 23	15 PAGE COUNT 19
16 SUPPLEMENTARY NOTATION					
17 COSATI CODES			18 SUBJECT TERMS (Continue on reverse if necessary and identify by block number)		
FIELD	GROUP	SUB-GROUP	Detection	Radar	
			Estimation	Doppler estimation	
19 ABSTRACT (Continue on reverse if necessary and identify by block number)					
<p>The maximum likelihood estimates of target Doppler frequencies after target detection in the presence of correlated nonstationary Gaussian noise are presented. The Cramer-Rao bounds on the Doppler for the nonstationary process are derived. It is found that in general the root-mean-square errors of the maximum likelihood estimates of the Doppler shift are very close to the Cramer-Rao bounds derived here.</p>					
20 DISTRIBUTION/AVAILABILITY OF ABSTRACT <input checked="" type="checkbox"/> UNCLASSIFIED/UNLIMITED <input type="checkbox"/> SAME AS RPT <input type="checkbox"/> DTIC USERS			21 ABSTRACT SECURITY CLASSIFICATION UNCLASSIFIED		
22a NAME OF RESPONSIBLE INDIVIDUAL F. C. Lin			22b TELEPHONE (include Area Code) (202) 767-3264		22c OFFICE SYMBOL 5340.1L

CONTENTS

INTRODUCTION	1
MAXIMUM LIKELIHOOD ESTIMATE	1
CRAMER-RAO BOUND	2
A RADAR ESTIMATION PROBLEM	4
EXAMPLE RESULTS	5
SUMMARY	5
REFERENCES	15

Accession For	
NTIS GRA&I	<input checked="" type="checkbox"/>
DTIC TAB	<input type="checkbox"/>
Unannounced	<input type="checkbox"/>
Justification	
By _____	
Distribution/	
Availability Codes	
Dist	Avail and/or Special
A-1	



BOUNDS ON DOPPLER FREQUENCY ESTIMATION IN CORRELATED NONSTATIONARY GAUSSIAN NOISE

INTRODUCTION

There exist many radar problems that require the detection of a signal in additive Gaussian noise. The optimal detector for this case is the classical matched filter, which is obtained by applying the Neyman-Pearson criteria to a binary hypothesis test [1]. For the pulsed radar problem of detecting a single Doppler-shifted target echo in a given range cell, there are three unknowns in the matched filter: the covariance matrix, the complex signal amplitude, and the target Doppler shift present in the steering vector. One practical detector is usually implemented as follows: the covariance matrix is estimated from data in nearby range cells [2]; a bank of Doppler filters or steering vectors is implemented so that the signal falls in one of them; finally, the magnitudes of all the Doppler filters are found and compared to a threshold. This final step eliminates the need to know the signal phase, and the signal magnitude is not required because the resulting test is uniformly most powerful. Reference 3 describes a variation of this procedure.

After detection, the Doppler shift of the target and its complex magnitude is estimated. Reference 4 gives the maximum likelihood estimate (MLE) of the complex magnitude, and the present report develops the estimation of the Doppler. The performance of the MLE of Doppler is studied for representative cases of interest that contain Gaussian noise composed of thermal noise plus clutter plus uncorrelated interference and a Doppler-shifted single point target. The performance of the MLE is then compared with that of the Cramer-Rao bound.

MAXIMUM LIKELIHOOD ESTIMATE

The received signal vector X , composed of n complex samples, is given by

$$X = N + bW,$$

where N is a complex zero-mean Gaussian process with covariance R , b is the unknown complex signal strength, and W is the steering vector. The steering vector is written in terms of Δ , the phase shift from pulse to pulse, owing to Doppler as

$$W^T = [1 \ e^{j\Delta} \ \dots \ e^{j(n-1)\Delta}],$$

where T denotes the transpose, and j is the square root of -1 . The joint probability density of X is then

$$p(X|\Theta) = \frac{1}{\pi^n |R|} \exp \{ -\overline{(X - bW)^T} R^{-1} (X - bW) \}, \quad (1)$$

where Θ represents the unknown parameters Δ , b , and \bar{b} , and $\overline{(\cdot)}$ denotes the complex conjugate. The MLEs of Δ , b , and \bar{b} are obtained by differentiating the likelihood density with respect to each of these variables, setting these resulting equations equal to zero, and solving for the three variables.

The MLEs of b and \bar{b} are well known [4] and are given by

$$b = \frac{\bar{W}^T R^{-1} X}{\bar{W}^T R^{-1} W} \quad (2)$$

and

$$\bar{b} = \frac{\bar{X}^T R^{-1} W}{\bar{W}^T R^{-1} W}. \quad (3)$$

The partial derivative of Eq. (1) with respect to Δ yields

$$(\bar{X} - b\bar{W})^T R^{-1} \left[b \frac{\partial W}{\partial \Delta} \right] + \left[\bar{b} \frac{\partial \bar{W}^T}{\partial \Delta} \right] R^{-1} (X - bW) = 0. \quad (4)$$

Substituting Eqs. (2) and (3) into Eq. (4) yields

$$\begin{aligned} & (\bar{W}^T R^{-1} W) (\bar{W}^T R^{-1} X) \left[\bar{W}^T R^{-1} \frac{\partial W}{\partial \Delta} \right] \\ & + (\bar{W}^T R^{-1} W) \left[\frac{\partial \bar{W}^T}{\partial \Delta} R^{-1} X \right] (\bar{X}^T R^{-1} W) \\ & - \left[\bar{W}^T R^{-1} \frac{\partial W}{\partial \Delta} \right] (\bar{W}^T R^{-1} X) (\bar{X}^T R^{-1} W) \\ & - \left[\frac{\partial \bar{W}^T}{\partial \Delta} R^{-1} W \right] (\bar{W}^T R^{-1} X) (\bar{X}^T R^{-1} W) = 0. \end{aligned}$$

which can be reduced by using the definition of W to

$$\sum_{i,k,l,m,p,q=1}^n (q - k + i - l) R_{ik}^{-1} R_{lm}^{-1} R_{pq}^{-1} e^{j\Delta(k-i+q-l)} X_m \bar{X}_p = 0. \quad (5)$$

The root of this polynomial that maximizes $p(X | \Theta)$ in Eq. (1) is the MLE of Δ .

CRAMER-RAO BOUND

The MLE is now compared to the Cramer-Rao bound [5,6]. The bound on the variance of Δ is obtained from the Fisher's information matrix J whose elements are

$$J_{ij} = E \left\{ \frac{\partial \ln p(X | \Theta)}{\partial \theta_i} \left[\frac{\partial \ln p(X | \Theta)}{\partial \theta_j} \right] \right\}, \quad (6)$$

where $\theta_1 = \Delta$, $\theta_2 = b$, and $\theta_3 = \bar{b}$; E is the expected value operator; and i and j are the indices. By using the density function (Eq. (1)) and the definition (Eq. (6)), then

$$J_{11} = b\bar{b} \frac{\partial \bar{W}^T}{\partial \Delta} R^{-1} \frac{\partial W}{\partial \Delta} + b\bar{b} \frac{\partial W^T}{\partial \Delta} R^{-1} \frac{\partial \bar{W}}{\partial \Delta},$$

$$J_{22} = W^T R^{-1} \bar{W} = C,$$

$$J_{33} = \bar{W}^T R^{-1} W = \bar{C},$$

$$J_{12} = b \frac{\partial W^T}{\partial \Delta} R^{-1} \bar{W} = bA,$$

$$J_{13} = \bar{b} \frac{\partial \bar{W}^T}{\partial \Delta} R^{-1} W = \bar{b}A,$$

$$J_{21} = \bar{b} W^T R^{-1} \frac{\partial \bar{W}}{\partial \Delta} = \bar{b} \frac{\partial \bar{W}^T}{\partial \Delta} R^{-1} W = \bar{b}A,$$

$$J_{31} = b \bar{W}^T R^{-1} \frac{\partial W}{\partial \Delta} = b \frac{\partial W^T}{\partial \Delta} R^{-1} \bar{W} = bA,$$

and

$$J_{23} = J_{32} = 0.$$

The matrix J can then be inverted in a closed form

$$J^{-1} = \frac{1}{|J|} \begin{bmatrix} C \bar{C} & -\bar{b}A\bar{C} & -bAC \\ -bAC & \bar{C}J_{11} - b\bar{b}A\bar{A} & b^2A^2 \\ -\bar{b}A\bar{C} & \bar{b}^2\bar{A}^2 & \bar{C}J_{11} - b\bar{b}A\bar{A} \end{bmatrix}^T, \quad (7)$$

where $|J|$, the determinant of the matrix J , is expressed by

$$|J| = C\bar{C}J_{11} - b\bar{b}A\bar{A}C - b\bar{b}A\bar{A}\bar{C}.$$

The bound on the variance of the estimate of Δ required by the Cramer-Rao bound is

$$\sigma_{\Delta}^2 \geq \frac{C\bar{C}}{|J|}, \quad (8)$$

which is the upper left-hand corner of the matrix given in Eq. (7).

A RADAR ESTIMATION PROBLEM

The covariance matrix R , composed of the sum of three covariance matrices, is written as

$$R = R_C + R_N + R_I,$$

where R_C , R_N , and R_I are the covariance matrices of clutter, thermal noise, and interference, respectively. For the examples to be studied these are given by

$$R_C = \sigma_C^2 \begin{bmatrix} 1 & \rho & \rho^2 & \cdot & \cdot & \rho^{n-1} \\ \rho & 1 & \rho & \cdot & \cdot & \rho^{n-2} \\ \rho^2 & \rho & 1 & \cdot & \cdot & \cdot \\ \cdot & \cdot & \cdot & \cdot & \cdot & \cdot \\ \rho^{n-1} & \rho^{n-2} & \cdot & \cdot & \rho & 1 \end{bmatrix},$$

$$R_N = \sigma_N^2 \begin{bmatrix} 1 & 0 & 0 & \cdot & \cdot & 0 \\ 0 & 1 & 0 & \cdot & \cdot & 0 \\ \cdot & \cdot & \cdot & \cdot & \cdot & \cdot \\ 0 & 0 & 0 & \cdot & \cdot & 1 \end{bmatrix},$$

and

$$R_I = \begin{bmatrix} \sigma_1^2 & 0 & 0 & \cdot & \cdot & 0 \\ 0 & \sigma_2^2 & 0 & \cdot & \cdot & 0 \\ \cdot & \cdot & \cdot & \cdot & \cdot & \cdot \\ 0 & 0 & 0 & \cdot & \cdot & \sigma_n^2 \end{bmatrix},$$

where σ_C , σ_N , and σ_i s are the standard deviations of the clutter, thermal noise, and the i th interference component, respectively, and ρ is the Markov correlation coefficient. The signal-to-noise ratio (SNR) is defined as

$$\text{SNR} = \frac{b\bar{b}}{\sigma_N^2}.$$

The performance of the MLE is evaluated by using simulation. Random numbers are generated according to the equation

$$X = N_N + N_C + N_I + |b| \exp(j\phi) W |_{\Delta=\Delta_0},$$

where W is evaluated at $\Delta = \Delta_0$, the true Doppler shift; N_N , N_I , and N_C are Gaussian-distributed complex vectors; and ϕ is a random phase distributed uniformly between 0 and 2π . The correlated clutter samples are generated from the uncorrelated Gaussian random numbers given by Z using

$$N_C = LZ,$$

where $R_C = LL^T$ and L is a lower triangular matrix. For the 3×3 cases,

$$L = \sigma_C \begin{bmatrix} 1 & 0 & 0 \\ \rho & \sqrt{1 - \rho^2} & 0 \\ \rho^2 & \rho\sqrt{1 - \rho^2} & \sqrt{1 - \rho^2} \end{bmatrix}.$$

These random numbers are used in Eq. (5) to obtain the MLE of Δ per trial. The variance of these estimates is then calculated by using a number of trials. The variances are normalized by $\frac{n\sigma_\Delta}{2\pi}$ and are plotted vs SNR in various clutter and interference environments.

The Cramer-Rao bounds of the normalized variances can also be obtained as a function of SNR for various cases. Equation (8) shows that the logarithm of the normalized Cramer-Rao bound is a linear function of SNR in dB.

EXAMPLE RESULTS

The results of the MLEs for the case of $n = 3$, $\rho = 0.999$, and $\sigma_C^2/\sigma_N^2 = 20$ dB without interference are shown in Figs. 1 and 2 (in dashed lines) for $\Delta = 0.1\pi$ and $\Delta = 0.5\pi$, respectively. These results are very close to the Cramer-Rao bounds (the solid lines in the figures) when the SNR is comparable to or above the clutter strength. Figures 3 through 7 show the results for the case where $n = 3$, $\rho = 0.999$, $\sigma_C^2/\sigma_N^2 = 20$ dB, and $\Delta = 0.5\pi$ in the presence of interference. Again, the MLE errors are tightly bounded by the Cramer-Rao bounds for SNR equal to or greater than the stronger of the clutter and the interference when only one pulse is subject to interference (Figs. 3 and 4). As the interference is applied to more than one pulse, the required SNR for the MLE errors to be close to the Cramer-Rao bounds is, generally, higher (Figs. 5 to 7).

Figure 8 shows the results for the case of $n = 5$, $\rho = 0.999$, and $\Delta = 0.5\pi$ without interference in the presence of clutter. The MLE errors are nearly identical to the Cramer-Rao bounds. Figure 9 shows the results for a clutter situation that has a clutter-to-noise ratio of 20 dB when interference is applied to both the first and the second pulses. Again the two methods yield very similar results.

SUMMARY

After detecting a radar target by use of a matched filter in the presence of clutter, thermal noise, and uncorrelated interference, the target Doppler shift is estimated. The MLE of Doppler and the associated Cramer-Rao bound were found for the Gaussian noise case. The estimation performance (variance of the estimate) was found for several cases of interest. The estimates were typically near the Cramer-Rao bound. In fact, they could be quite close even in the presence of high clutter and interference.

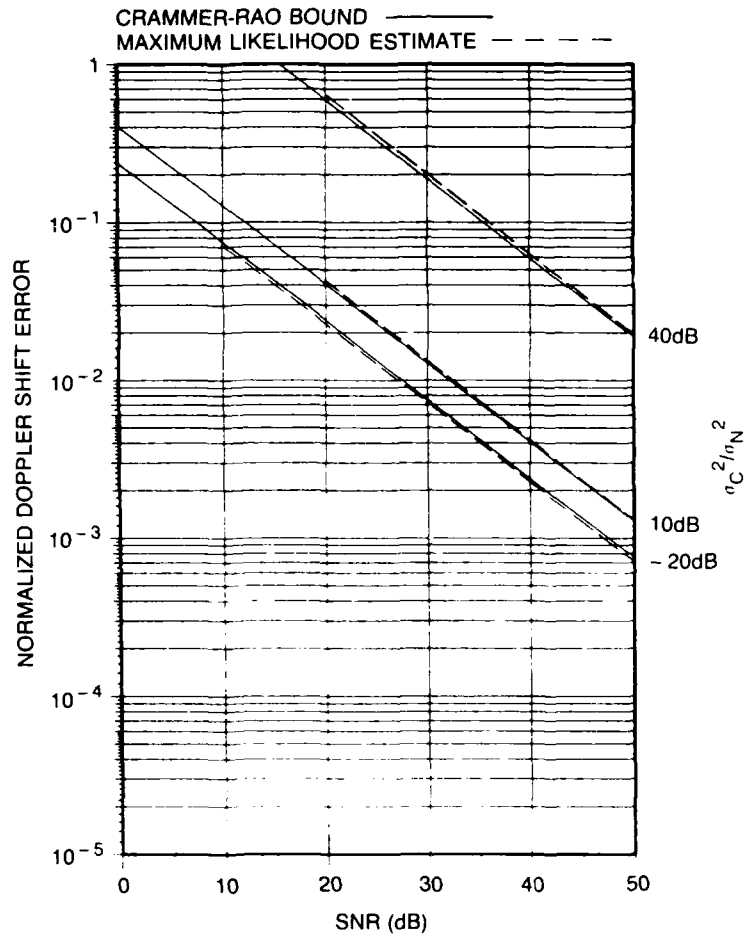


Fig. 1 — The bounds and the maximum likelihood estimates of normalized Doppler shift errors vs SNR for $n = 3$, $\rho = 0.999$, and $\Delta = 0.1 \pi$ without interference in clutter

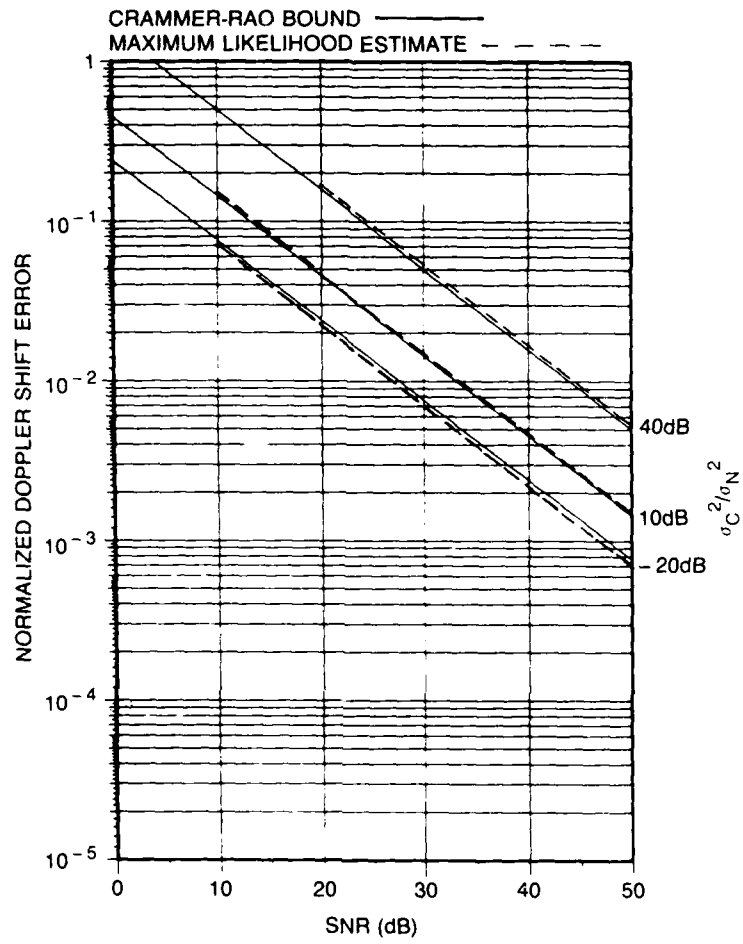


Fig. 2 — The bounds and the maximum likelihood estimates of normalized Doppler shift errors vs SNR for $n = 3$, $\rho = 0.999$, and $\Delta = 0.5\pi$ without interference in clutter

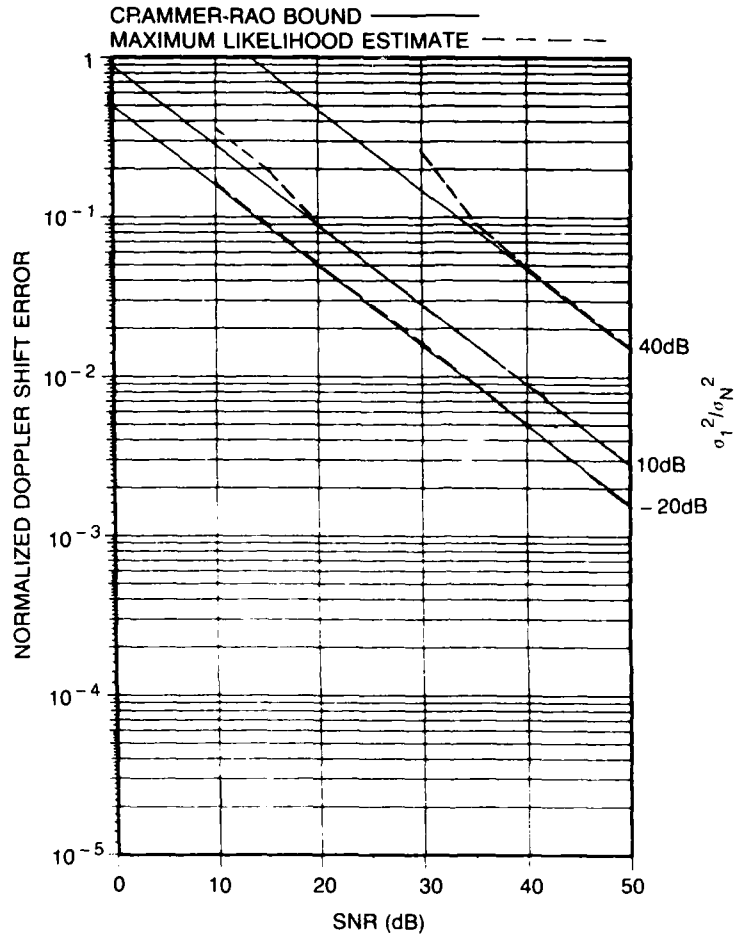


Fig. 3 — The bounds and the maximum likelihood estimates of normalized Doppler shift errors vs SNR for $n = 3$, $\rho = 0.999$, $\Delta = 0.5\pi$, and $\sigma_c^2/\sigma_w^2 = 20$ dB with interference on the first pulse

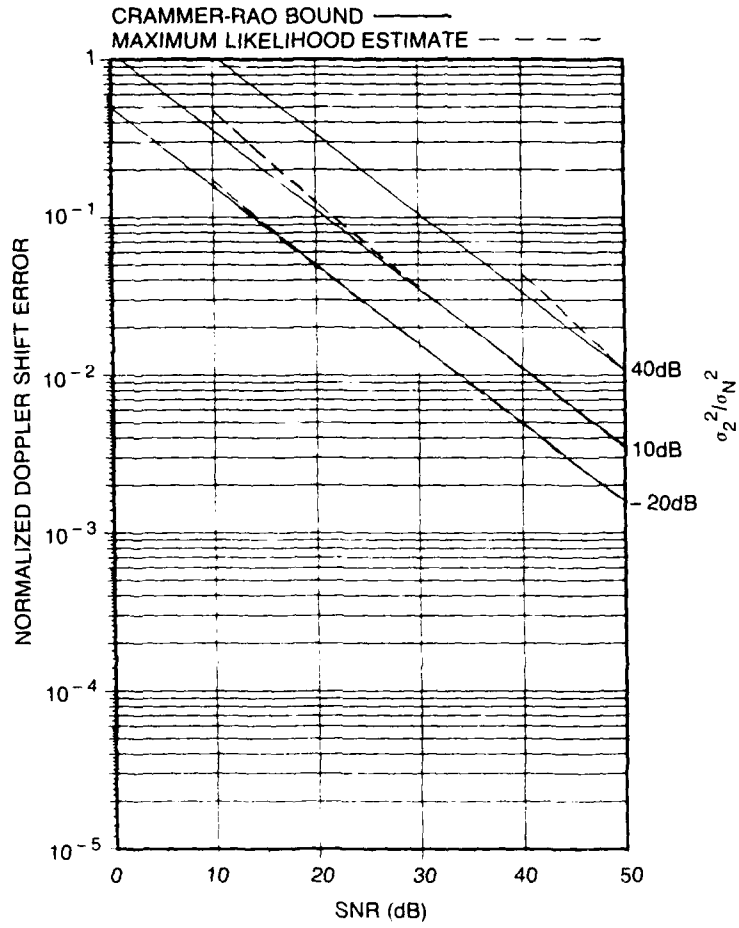


Fig. 4 — The bounds and the maximum likelihood estimates of normalized Doppler shift errors vs SNR for $n = 3$, $\rho = 0.999$, $\Delta = 0.5\pi$, and $\sigma_c^2/\sigma_N^2 = 20$ dB with interference on the second pulse

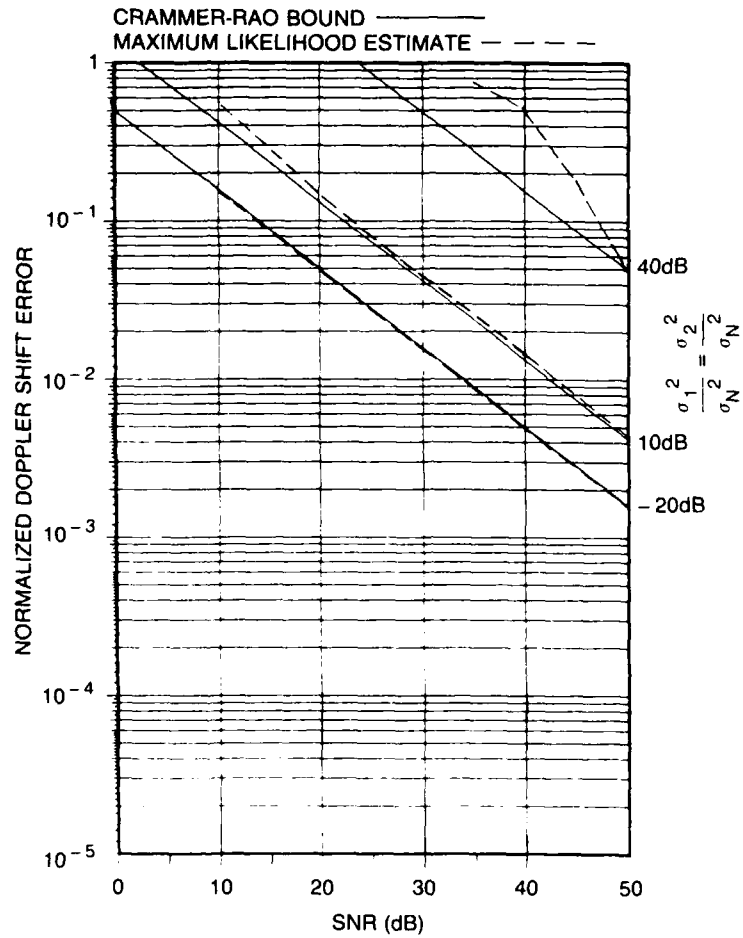


Fig. 5 — The bounds and the maximum likelihood estimates of normalized Doppler shift errors vs SNR for $n = 3$, $\rho = 0.999$, $\Delta = 0.5\pi$, and $\sigma_c^2/\sigma_N^2 = 20$ dB with interference on the first and the second pulses

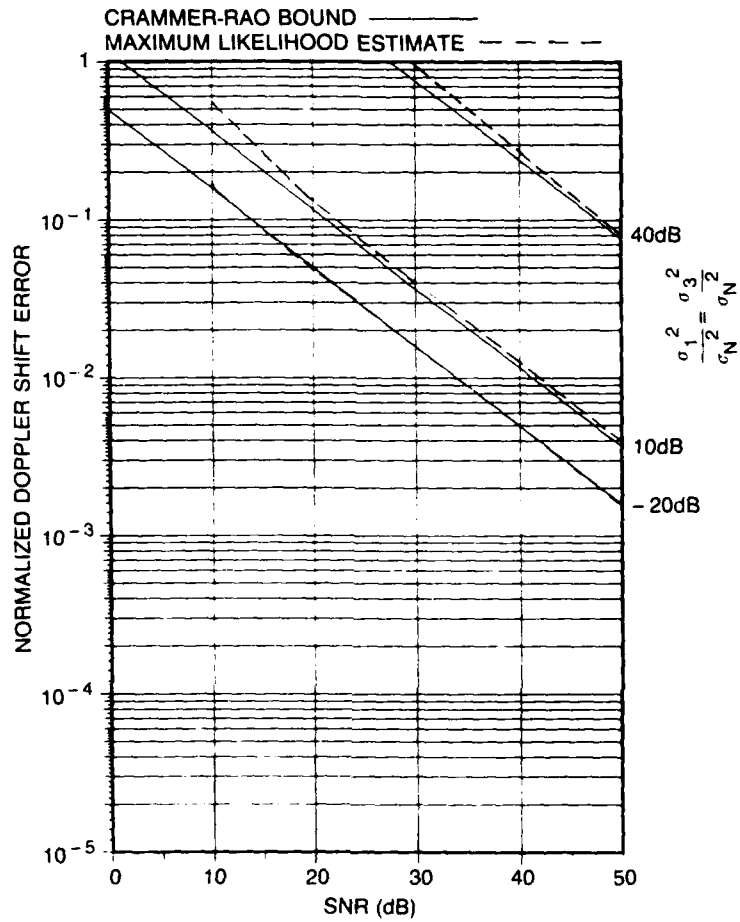


Fig. 6 — The bounds and the maximum likelihood estimates of normalized Doppler shift errors vs SNR for $n = 3$, $\rho = 0.999$, $\Delta = 0.5\pi$, and $\sigma_c^2/\sigma_N^2 = 20$ dB with interference on the first and the third pulses

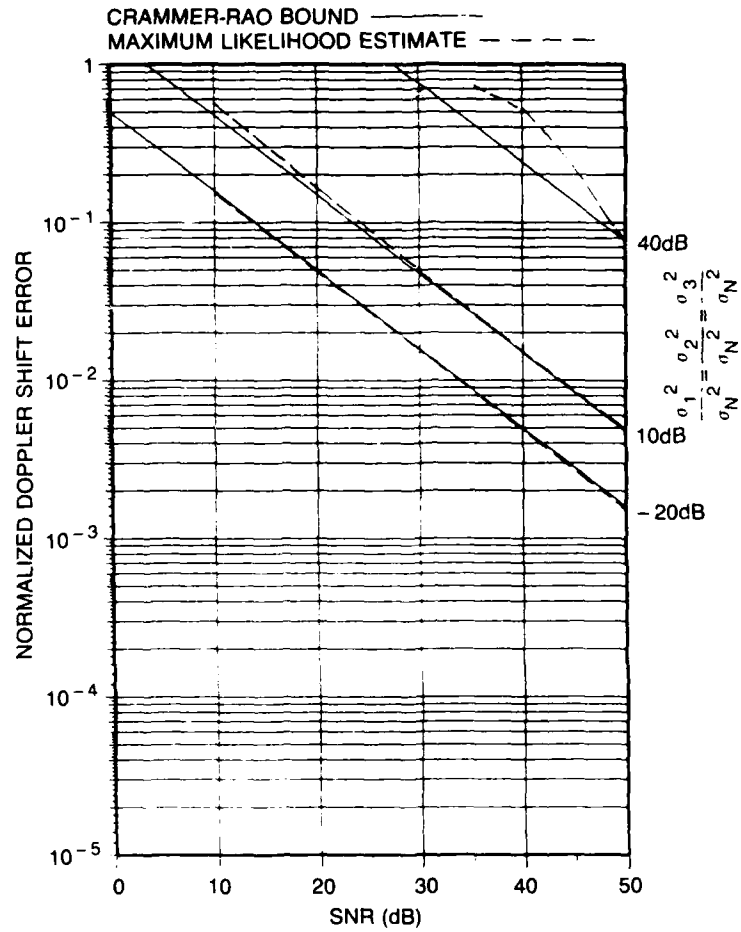


Fig. 7 — The bounds and the maximum likelihood estimates of normalized Doppler shift errors vs SNR for $n = 3$, $\rho = 0.999$, $\Delta = 0.5\pi$, and $\sigma_c^2/\sigma_N^2 = 20$ dB with interference on all pulses

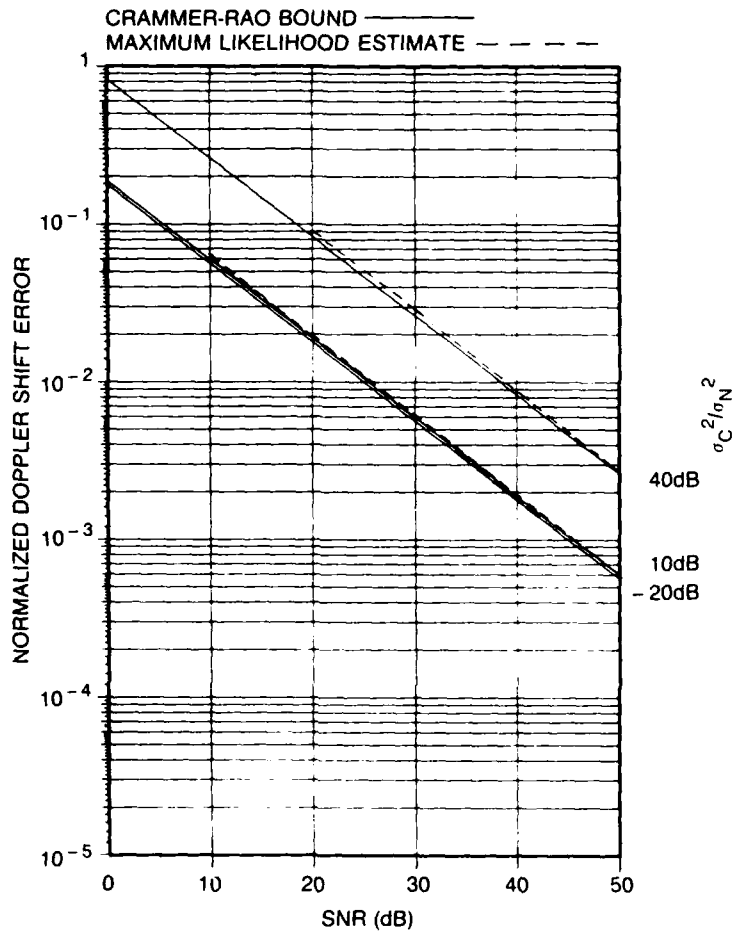


Fig. 8 — The bounds and the maximum likelihood estimates of normalized Doppler shift errors vs SNR for $n = 5$, $\rho = 0.999$, and $\Delta = 0.5\pi$ without interference in clutter

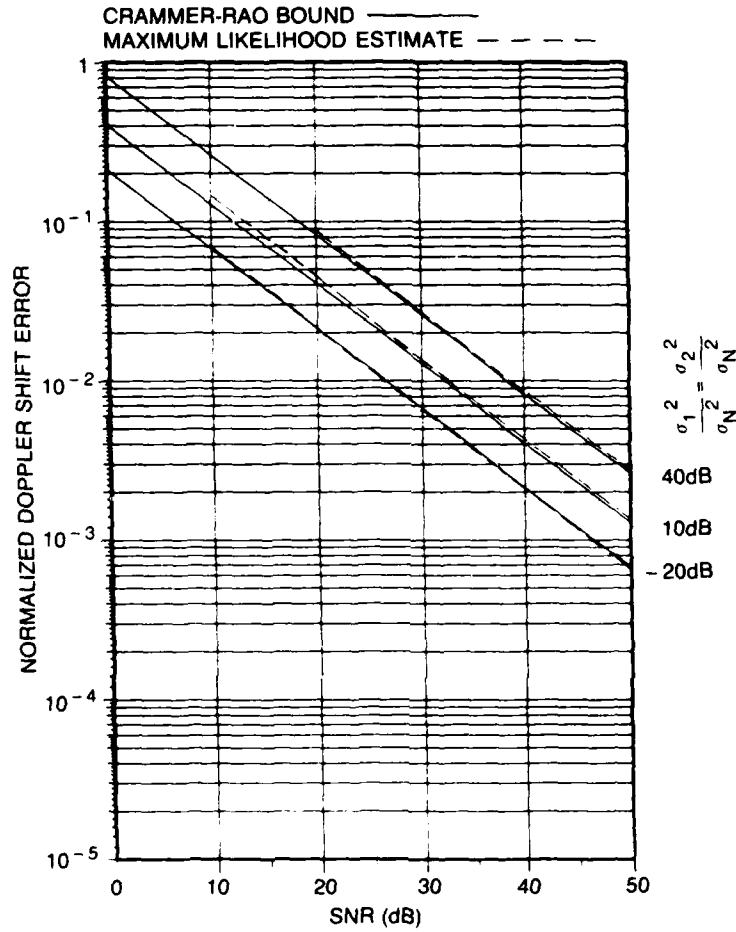


Fig. 9 — The bounds and the maximum likelihood estimates of normalized Doppler shift errors vs SNR for $n \approx 5$, $\rho = 0.999$, $\Delta = 0.5\pi$, and $\sigma_1^2/\sigma_2^2 = 20$ dB with interference on the 1st and the 2nd pulses

REFERENCES

1. H.L. Van Trees, *Detection, Estimation, and Modulation Theory: Part I* (Wiley, New York, 1968), Ch. 2.
2. N.R. Goodman, "Statistical Analysis Based on Certain Multivariate Complex Processes," *Ann. Math. Stat.* **34**, 152-177 (1963).
3. E.J. Kelly, "An Adaptive Detection Algorithm," *IEEE Trans. Aerosp. Electron. Syst.* **AES-22**, 115-127, March 1986.
4. K.S. Miller, *Complex Stochastic Processes* (Addison-Wesley Publishing Co., Reading, MA, 1974).
5. H. Cramer, *Mathematical Methods of Statistics* (Princeton University, Princeton, N.J., 1951), Ch. 22-23.
6. C.R. Rao, *Linear Statistical Inference and Its Application* (Wiley, New York, 1965), Ch. 5.